JOURNAL
OF THE AMERICAN CHEMICAL SOCIETY

VOLUME 99, NUMBER 9 APRIL 27, 1977

Study of *n*-Type Semiconducting Cadmium Chalcogenide-Based Photoelectrochemical Cells Employing Polychalcogenide Electrolytes

Arthur B. Ellis,[1] Steven W. Kaiser, Jeffrey M. Bolts, and Mark S. Wrighton*[2]

Contribution from the Department of Chemistry, Massachusetts Institute of Technology, Cambridge, Massachusetts 02139. *Received August 27, 1976*

Abstract: Studies of CdX-based photoelectrochemical cells in X^{2-}/X_n^{2-} electrolytes are reported for X = S, Se, and Te. For eight of the nine electrode/electrolyte combinations we have demonstrated that the *n*-type semiconducting single-crystal CdX photoelectrodes are stable to anodic dissolution. Only for CdTe in S^{2-}/S_n^{2-} do we find that oxidation of the added chalcogenide does not quench the decomposition of CdX typically found in aqueous electrolytes. For all eight remaining electrolyte/electrode combinations the added chalcogenide is oxidized at the photoelectrode at a rate which precludes anodic dissolution of the CdX. For the stable combinations each electrolyte is capable of being oxidized at the photoelectrode and subsequently reduced at the dark counter electrode to complete a cycle where no net chemical change obtains. For all nine electrolyte/electrode combinations and for the CdX in alkaline H_2O, the redox level associated with the oxidation of X^{2-} or with O_2 evolution is between the valence band and conduction band positions at the semiconductor-electrolyte interface. Thus, energetic requirements for X^{2-} oxidation or O_2 evolution from H_2O are met in all cases, but apparently kinetic factors control whether oxidation of X^{2-} or of H_2O will be fast compared to anodic dissolution, which is also energetically feasible. For the stable electrode/electrolyte combinations, conversion of optical to electrical energy can be accomplished with efficiencies of >10% for monochromatic visible light. For CdTe or CdSe in the Te^{2-}/Te_2^{2-} electrolyte input power densities of >500 mW/cm^2 can be converted with a few percent efficiency with no deterioration of properties. Output voltages at maximum power conversion efficiency are of the order of 0.4 V.

Sustained, efficient conversion of low energy visible light to electricity has recently been demonstrated using photoelectrochemical cells like that depicted in Scheme I.[3-6] A key element of the recent discoveries is that the reversible redox systems employed not only result in no net chemical change in the electrolyte, but also stabilize the *n*-type semiconductor photoelectrode to anodic dissolution. Presumably, the electrolyte additive is capable of undergoing photoinduced oxidation[3-7] at the semiconductor electrode at a rate which completely overwhelms the general photoanodic dissolution reaction[8] of the small band gap *n*-type semiconductors.

Scheme I. Photoelectrochemical Cell for Conversion of Light to Electricity

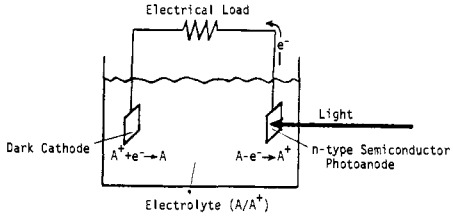

The only *n*-type materials that have been characterized and established as inherently stable to photoanodic dissolution in aqueous electrolytes are WO_3,[9] TiO_2,[10-20] $SrTiO_3$,[21-23] SnO_2,[24] $KTaO_3$,[25] and $KTa_{0.77}Nb_{0.23}O_3$.[25] All of these metal oxides have large band gaps and consequently, according to the model[26] for semiconductor photoelectrodes, do not respond to low-energy visible light. If the aim in such systems is to photoelectrolyze H_2O, lowering the band gap may jeopardize stability or current-voltage properties.[27] To not lower band gap dooms such systems to low efficiencies.

Our studies[3-6] of *n*-type CdS (band gap = 2.4 eV),[28] CdSe (band gap = 1.7 eV),[29] and CdTe (band gap = 1.4 eV)[30] show that it is possible to find redox systems which stabilize small band gap electrodes which generally undergo photoanodic dissolution. However, the factors influencing the choice of the redox system are not yet elucidated. For example, why does the S^{2-}/S_n^{2-} electrolyte fail[6] to stabilize CdTe, whereas CdSe is completely stabilized? Importantly, the S^{2-}/S_n^{2-} redox potential apparently falls between the position of the conduction band (CB) and valence band (VB) of both CdSe and CdTe, as theoretically required.[26]

The aim of the present paper is to complete the preliminary characterization[6] of the *n*-type CdTe-based photoelectrochemical cell employing the Te^{2-}/Te_2^{2-} electrolyte. Additionally, we report new studies on *n*-type CdX-based cells using X^{2-}/X_n^{2-} electrolytes for X = S, Se, and Te. From differential capacitance measurements, open-circuit photopotential, and onset potential of photoanodic current we have made estimates of the CB and VB positions for each of the three CdX electrodes in each of the three X^{2-}/X_n^{2-} electrolytes. The results reveal that factors other than energetics alone control whether the X^{2-}/X_n^{2-} electrolyte quenches the photoanodic

Table I. Stabilization of *n*-Type CdX Photoelectrodes in X/X^{2-} Electrolytes

Crystal[a]	Initial electrolyte (T, °C)[b]	Crystal before,[c] mol × 10^4	Crystal after,[c] mol × 10^4	Electrons,[d] mol × 10^4	Av i, mA[e]	V_{appl}[f]	t, h	Irradiation source[g]
CdTe	0.18 M Te^{2-} (51)	4.05_0	4.05	1.64	0.94	−0.20	4.67	633 nm
CdTe	0.03 M Se^{2-} (35)	4.77	4.76	6.62	0.72_5	0.00	24.5	633 nm
CdSe	0.02 M Te^{2-} (25)	7.09	7.10	2.82	0.36	0.00	21.0	Tungsten
CdSe	0.03 M Se^{2-} (35)	9.09	9.09	7.17	0.42_5	0.00	45.2	Tungsten
CdS	0.03 M Se^{2-} (35)	4.81	4.82	1.73	0.10	0.00	45.2	Tungsten
CdS	0.10 M Te^{2-} (60)	8.46	8.42	11.0	1.65	−0.05	17.9	Hg

[a] Crystals were *n*-type semiconductors approximately 5 × 5 × 1 mm supplied as single crystals by Cleveland Crystals, Inc. Resistivities of ~1-20 Ω-cm were typical. [b] Electrolyte was 5.0 M NaOH plus the indicated X^{2-} ion added as the Na^+ salt. All experiments are for stirred electrolytes under Ar. During electrolysis the X^{2-} species is oxidized to polychalcogenide ions. [c] Crystal moles determined by weight before and after photoelectrochemistry. [d] Moles of electrons determined by integrating photocurrent vs. time plot. [e] In no experiment did photocurrent drop more than 5% for reasons other than changes in optical density of the electrolyte associated with the $nX^{2-} \rightarrow X_n^{2-}$ reaction. For current density multiply by ~4 cm^{-2}. [f] Applied potential from external power supply in series with Pt cathode and CdX photoanode. Negative value indicates that the power supply represents an electrical load (negative lead of power supply to photoanode) and 0.00 V applied indicates that CdX is merely short-circuited to Pt. [g] The irradiation source indicated by 633 nm is a 6× beam-expanded He-Ne laser with ~3 mW of uniform irradiation on the photoelectrode. The tungsten source is the full output from a 650-W tungsten-halogen lamp, and Hg is a UV-filtered 200-W Hg source.

dissolution of *n*-type CdX photoelectrodes. Measures of energy conversion efficiency for all nine systems show that the CdTe-based photoelectrochemical cell employing a Te^{2-}/Te_2^{2-} electrolyte yields the most efficient conversion of optical to electrical power.

Results and Discussion

In the sections below we outline our results on the electrode reactions occurring in a cell consisting of a Pt-gauze cathode and a CdX anode in a stirred X/X^{2-} electrolyte under Ar. For several new combinations of electrolyte and CdX we find that the CdX does not undergo detectable photoanodic dissolution. The essential new results concerning stability are summarized in Table I. Stability is crucial, since it allows a meaningful determination of other properties such as current-voltage behavior, wavelength response, photopotential, energy conversion properties, and CdX band positions at the surface exposed to the electrolyte. Results pertaining to the electrode reactions are presented first, and these are followed by our findings concerning the other properties. In the final section we provide some data which show that the instability of CdTe in the S^{2-}/S_n^{2-} electrolyte is only understandable in terms of kinetic factors rather than energetics.

a. Stabilization of CdX Photoanodes: Cathode and Photoanode Reactions in X^{2-}/X_n^{2-} Electrolytes. Irradiation of an *n*-type semiconductor CdX electrode in a cell with a Pt dark electrode using light of wavelength equal to or shorter than that corresponding to the band gap energy, E_{BG}, results in current flow such that electrons flow toward the Pt electrode. It is now well documented[3-8] that in aqueous electrolytes the electron flow corresponds to the photoanodic dissolution of CdX according to the reaction

$$\underset{\text{(photoanode)}}{CdX} \xrightarrow{\text{light}} Cd^{2+} + X + 2e^- \qquad (1)$$

X = S, Se, Te

Indeed, in our hands, in an aqueous 5.0 M NaOH electrolyte we easily visually detect a film of X on CdX photoelectrodes after short irradiation times. The typical result is that the photocurrent declines rapidly in time, and with the current that does flow the CdX is stoichiometrically and irreversibly consumed. The reduction occurring at the Pt dark electrode is the reduction of H_2O to yield H_2 gas.

Addition of certain redox active species to the aqueous alkaline electrolyte effectively quenches reaction 1, since oxidation of the added species could occur at a rate which would preclude the decomposition of the electrode. To determine whether the electrode is stable in a given electrolyte we have applied two criteria: (i) is the photocurrent constant in time? and (ii) is there weight loss (or other obvious deterioration) of the CdX during the passage of photocurrent? Stable photocurrents and constant weight electrodes provide unequivocal assurance that the electrodes are inert to photoanodic dissolution.

Table I summarizes measurements of stability for CdX under various conditions. No details are given for the CdTe electrode in the S^{2-}-containing electrolyte, since we find this combination to be unstable. Irradiation (633 nm, 12 mW/cm^2) of the CdTe (potentiostated at −0.9 V vs. SCE) in 1 M NaOH/1 M Na_2S results in the obvious formation of an insoluble orange-yellow material on the surface of the CdTe. The orange-yellow film is apparently CdS from photoanodic dissolution followed by precipitation of the Cd^{2+} ions by the S^{2-} in the electrolyte. Irradiation of CdTe electrodes in 1 M NaOH/1 M Na_2S/1 M S, under similar conditions, results in a rapid decline in photocurrent which is apparently due to the photoanodic decomposition of the CdTe. The behavior of the various electrolyte/electrode combinations is discussed below.

1. S^{2-}/S_n^{2-} Electrolyte. We previously reported[3-5] the behavior of single-crystal CdS and CdSe electrodes in an electrolyte consisting of 1.0 M NaOH, 1.0 M Na_2S, and 1.0 M S. The photoanodic dissolution does not occur and the electrode reactions are the oxidation of S_n^{2-} species at the photoanode and the reduction of the S_n^{2-} species at the Pt dark electrode. As described above, and noted earlier,[6] we find that the oxidation of S_n^{2-} does not occur rapidly enough to quench the photoanodic dissolution of CdTe.

A recent communication[7] describes the behavior of a polycrystalline CdSe electrode in the same electrolyte. Stabilization was claimed, but the presence of a small amount of CdS on the CdSe surface was noted. This result leaves one with the impression that the S^{2-}/S_n^{2-} electrolyte will only stabilize CdS, and possibly that the mechanism of stabilization is rapid precipitation of CdS by reaction of Cd^{2+} with S^{2-}. Such may be the case for the polycrystalline sample of CdSe run at the current densities reported,[7] but for the single-crystal CdS and CdSe samples we have studied[3-5] we conclude that the CdSe is indeed stabilized by S^{2-}/S_n^{2-} and that the mechanism involves fast oxidation of the *added* S_n^{2-}. However, the photoanodic decomposition of CdTe, by comparison to CdSe, is obvious in the S^{2-}/S_n^{2} electrolyte.

2. Te^{2-}/Te_2^{2-} Electrolyte. An electrolyte initially consisting of 0.03-0.18 M Na_2Te in aqueous 5.0 M NaOH can be used

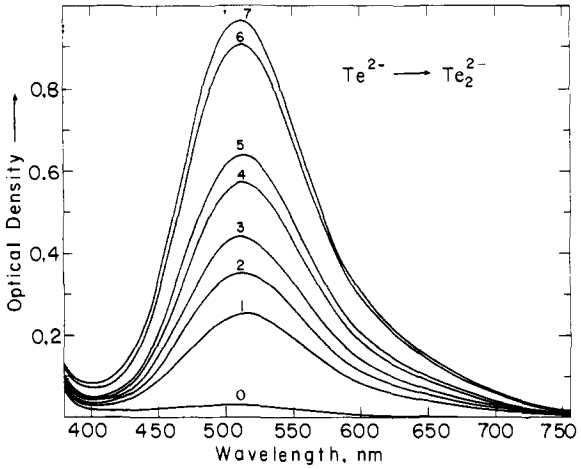

Figure 1. Spectral changes accompanying the electrolysis of 0.03 M Na_2Te in 5.0 M NaOH aqueous solution under Ar. The total solution volume is 2.0 cm^3 and the optical path length is 0.1 cm. The electrolysis is carried out by applying a 0.5 V potential between two Pt gauze electrodes. Curve 0 is the initial spectrum and curves 1, 2, 3, 4, 5, 6, and 7 are after the passage of 7.90, 14.90, 21.84, 50.6, 80.0, 950, and 2300 μmol of electrons. The peak at 512 nm is associated with Te_2^{2-}.

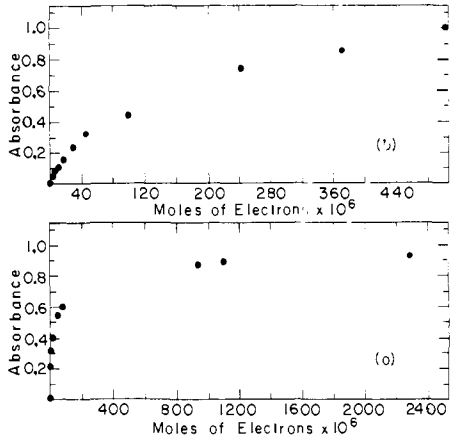

Figure 2. (a) Plot of optical density vs. electrons passed in electrolysis described in Figure 1 showing the leveling off of Te_2^{2-} formation. (b) Plot of optical density associated with Te_2^{2-} formed in a CdTe-based photoelectrochemical cell initially containing 0.03 M Na_2Te in 5.0 M NaOH. Irradiation was carried out at 633 nm. The leveling in a and b is associated with achievement of constant Te^{2-}/Te_2^{2-} composition.

to quench the photoanodic dissolution of CdS, CdSe, and CdTe, Table I. Though CdS is stabilized under the conditions given in Table I, we note that at a significantly lower Te^{2-} concentration we were unable to completely quench the decomposition. Initially colorless, or nearly colorless, solutions containing Te^{2-} rapidly became purple upon irradiation of the CdX electrodes. Indeed, under intense irradiation, a stream of purple color can be easily seen evolving from the photoelectrode. Initially, H_2 gas is evolved from the dark Pt electrode, but after some purple color is generated the H_2 evolution slows and ultimately no gas generation is detectable. Experimentally, of course, the increasing purple color results in lower photocurrents, since a fraction of the incident 633-nm light is absorbed by the electrolyte. After correction for light absorption by the electrolyte, photocurrents are invariant in time for densities in the range of 10 mA/cm^2. Higher current densities have been sustained, vide infra, with no deterioration of the CdX photoanodes in the Te^{2-}/Te_2^{2-} electrolyte.

The purple color generated at the photoanode is associated with the oxidation of Te^{2-}, which ultimately results in the formation of Te_2^{2-}.[31] As the Te_2^{2-} concentration builds up it becomes possible to reduce Te_2^{2-} back to Te^{2-} at the cathode. That is, the set of equations (2 and 3) describes the cell processes in the Te^{2-}/Te_2^{2-} electrolyte.

$$\left.\begin{aligned} 2Te^{2-} &\rightarrow Te_2^{2-} + 2e^- \\ \text{or} \qquad Te_2^{2-} + 2Te^{2-} &\rightarrow 2Te_2^{2-} + 2e^- \end{aligned}\right\} \text{(anode)} \qquad (2)$$

$$Te_2^{2-} + 2e^- \rightarrow 2Te^{2-} \text{ (cathode)} \qquad (3)$$

We have done experiments with the CdTe-based photoelectrochemical cell and with a conventional cell (two Pt electrodes and a power supply) to determine the electrochemical stability of the Te^{2-}/Te_2^{2-} electrolyte and to establish reactions 2 and 3. First, we will describe the behavior of the two Pt electrode cell. Applying a potential of 0.5 V between two Pt electrodes in 2.0 mL of an electrolyte initially consisting of 0.03 M Na_2Te in aqueous 5.0 M NaOH results in significant current flow (~1 mA). Gas evolution (H_2) is initially observed at the cathode and purple color is generated at the anode. Spectral changes accompanying such an electrolysis in a 0.1-cm path-length cuvette sealed under Ar are shown in Figure 1, and the optical density at 512 nm as a function of time is shown in Figure 2a. During the electrolysis the current was measured continuously. Thus, spectral changes could be related to electrical equivalents. Initially, we found that for every 4 μmol of electrons the optical density increased 0.1 absorbance units at 512 nm under our conditions. Assuming that the oxidation of Te^{2-} quantitatively generated Te_2^{2-}, the molar absorptivity of Te_2^{2-} at 512 nm was calculated to be ~1000 L mol^{-1} cm^{-1}. The rapid increase in absorbance due to Te_2^{2-} falls off and we note a concomitant decline in gas evolution at the cathode. Finally, passage of current results in no further spectral changes. Moreover, the current remains constant (at constant applied potential). During the period when no further spectral changes obtained, enough current was passed to cycle $2Te^{2-} \rightleftarrows Te_2^{2-}$ over 15 times. This justifies our assumption concerning the quantitative nature of the oxidation of Te^{2-}. Thus, the experiment with a conventional electrolysis cell shows that, under a given set of conditions, the Te^{2-} electrolyte will ultimately reach steady-state amounts of Te^{2-} and Te_2^{2-}. Usually, our major difficulty in maintaining the equilibrium is an inability to rigorously exclude O_2, which rapidly oxidizes Te^{2-} to Te_2^{2-} and Te_2^{2-} to Te.

The spectral changes and current accompanying the irradiation of a CdTe anode in a cell with 0.03 M Na_2Te in aqueous 5.0 M NaOH were also monitored. In Figure 2b we plot the optical density at 600 nm as a function of photoelectrolysis time. After initial, rapid generation of Te_2^{2-} the optical density changes become smaller and a steady-state ratio of Te^{2-} and Te_2^{2-} is ultimately achieved. Again, during the period of irradiation enough photocurrent passed to cycle $2Te^{2-} \rightleftarrows Te_2^{2-}$ a significant number of times. Except for variation due to optical density changes, the photocurrent was constant and there was no weight loss in the CdTe. Spectral changes found for photoelectrolysis are in agreement with the conventional electrolysis results, and this convinces us that the electrochemistry in either the conventional cell or the photoelectrochemical cell is adequately represented by eq 2 and 3.

One final point concerning the Te^{2-}/Te_2^{2-} electrolyte relates to the observation of a Te film on CdX electrodes exposed to intense irradiation. At high light intensity and at the lower concentrations of Te^{2-}, we note that it is possible to observe the formation of a Te film on either CdSe or CdTe. The Te film is dissolved off rapidly by the Te^{2-} electrolyte, generating the Te_2^{2-} if the light is turned off. The film formation provides a rationale for the fact that at high light intensities the photocurrent immediately upon exposure is higher than the steady state, constant photocurrent. We questioned whether such a

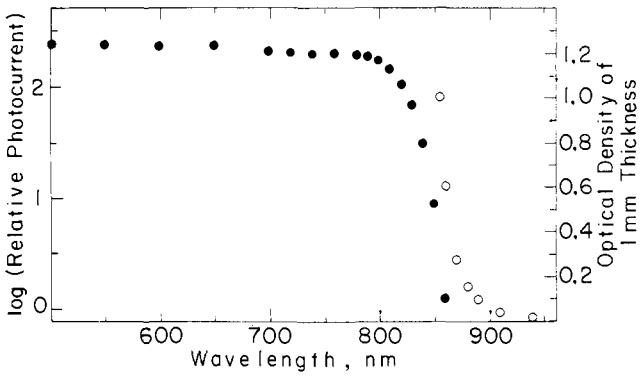

Figure 3. Optical density (right scale and ○) of a 1-mm thick sample of optically polished CdTe, and relative photocurrent (left scale and ●) vs. wavelength for a CdTe-based photoelectrochemical cell. Relative photocurrents shown have been corrected for variation in light intensity with wavelength.

Te film could in fact be responsible for the observed stability of the CdSe and CdTe electrodes. Consequently, we used an electrolyte containing initially 0.18 M Te^{2-} and increased the temperature to 49 °C to more rapidly remove the Te from the CdX surface. Under these conditions no steady-state film formation was observable, and the instantaneous and steady-state photocurrents were the same. Thus, we are convinced that the stability of CdSe and CdTe in the Te^{2-}/Te_2^{2-} electrolyte is a consequence of rapid oxidation of the added Te^{2-} or Te_2^{2-}.

3. Se^{2-}/Se_n^{2-} Electrolyte. An electrolyte initially consisting of $\sim 10^{-2}$ M Na_2Se and 5.0 M NaOH in H_2O is also capable of stabilizing all three CdX photoelectrodes, Table I. As for Na_2Te, the Na_2Se is initially colorless, but becomes colored with the passage of current. Oxidation of Se^{2-} to zerovalent Se obtains at the anode, and initially, at least, gas evolution (H_2) occurs at the dark cathode. But ultimately, again, gas evolution ceases and apparently the cyclic oxidation and reduction of polyselenide species occurs. For the Se^{2-}/Se_n^{2-} system the identity of the Se_n^{2-} species is less certain than in the case of Te^{2-}/Te_2^{2-}. However, electrolysis of 5×10^{-3} M Se^{2-} in 5.0 M NaOH with two Pt electrodes yields clean, monotonic spectral changes similar to those in Figure 2 for the Te^{2-}. A visible absorption band grows at ~425 nm which is associated with the Se_n^{2-} species. As for the Te^{2-} electrolyte, spectral changes stop concomitant with cessation of gas evolution at the cathode. This reflects the fact that the cathode reaction becomes the reduction of Se_n^{2-}. The clean, uniform spectral changes accompanying the electrolysis of Se^{2-} are consistent with postulating that the Se_n^{2-} species is in fact Se_2^{2-} under these conditions. However, there is no certain assignment[32] of the 425-nm band as being due to Se_2^{2-}. Assuming that it is Se_2^{2-}, the absorptivity of Se_2^{2-} at 425 nm is ~ 1000 L mol^{-1} cm^{-1}.

A plot of absorbance at 425 nm as a function of electrolysis time reveals that one can establish a steady-state ratio Se^{2-}/Se_n^{2-} and that $Se^{2-} \rightleftarrows Se_n^{2-}$ can be cycled a number of times without deterioration. Comparable results are obtained using photoelectrochemical cells and good agreement on the absorptivity of Se_2^{2-} is found. Thus, we represent the cell reactions by the equations

$$n\mathrm{Se}^{2-} \rightarrow \mathrm{Se}_n^{2-} + 2(n-1)\mathrm{e}^- \text{ (anode)} \quad (4)$$

$$\mathrm{Se}_n^{2-} + 2(n-1)\mathrm{e}^- \rightarrow n\mathrm{Se}^{2-} \text{ (cathode)} \quad (5)$$

b. Wavelength Response of CdX and Electrolyte Absorption. We have previously reported[4,5] the wavelength response of CdS and CdSe in the sulfide-containing electrolyte. The essential features of such curves are independent of the electrolyte in the sense that a large increase in photocurrent is found as the excitation wavelength moves through the range corresponding to E_{BG} of the material. Thus, a sharp increase of photocurrent for CdS and CdSe is found near 515 (E_{BG} = 2.4 eV)[28] and 730

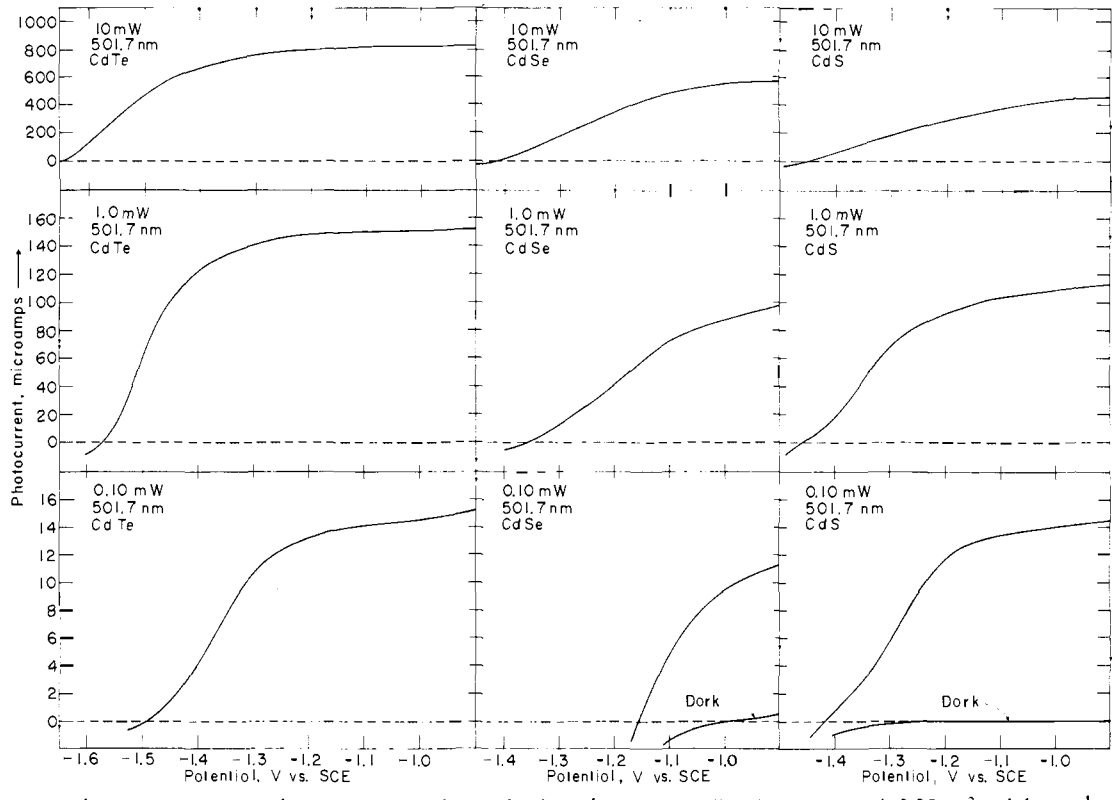

Figure 4. Current–voltage curves for CdX electrodes in the Se^{2-}/Se_n^{2-} electrolyte. The irradiated surface area is 0.25 cm^2 and the total concentration of Se is $\sim 10^{-2}$ M in 5.0 M NaOH. The Pt dark electrode was at a constant potential of −0.95 V vs. SCE (Se^{2-}/Se_n^{2-} potential) for all values of potential shown for the CdX electrode. Note the dependence on light intensity. These are potentiostated curves recorded at 2 mV/s.

nm (E_{BG} = 1.7 eV),[29] respectively. For CdTe the wavelength response and absorption of a 1.0-mm thick sample are shown in Figure 3. As expected, the sharp increase in photocurrent (~860 nm) and the absorption edge correspond closely to one another and the known E_{BG} of 1.4 eV.[30]

All three X^{2-}/X_n^{2-} electrolytes have significant absorption in the visible region. The spectral features of the Te^{2-}/Te_2^{2-} and Se^{2-}/Se_n^{2-} systems were mentioned above. The absorbance of our usual polysulfide electrolyte (1.0 M NaOH, 1.0 M Na_2S, 1.0 M S) is large for wavelengths shorter than ~500 nm. Importantly, for short path lengths each electrolyte transmits a significant fraction of the entire visible spectrum.

c. Current-Voltage Properties and Energy Conversion Efficiencies. Since neither the CdX nor the X^{2-}/X_n^{2-} electrolyte suffers any deterioration, with the exception of CdTe in S^{2-}/S_n^{2-}, it may be possible to sustain conversion of input optical energy to electrical energy. The efficiency of the conversion depends on a number of factors including the photocurrent-voltage properties and quantum efficiency. Ideally, one would seek a quantum efficiency for electron flow, Φ_e, of unity at E_{BG}. Deviations from these ideal outputs naturally contribute to inefficiency. In this section we report our results on current-voltage behavior and quantum efficiency.

1. Current-Voltage Curves with Potentiostated CdX Electrodes. We have already reported[4,5] the current-voltage behavior of CdS and CdSe in the 1.0 M NaOH, 1.0 M Na_2S, 1.0 M S electrolyte. We show in Figure 4 the current-voltage behavior of CdX (X = S, Se, Te) in the Se^{2-}/Se_n^{2-} electrolyte, and in Figure 5 we show the current-voltage behavior of CdSe and CdTe in the Te^{2-}/Te_2^{2-} electrolyte. Data are given at three light intensities for each electrode/electrolyte combination. In each case the potential of the photoelectrode is given vs. the SCE, and positive currents correspond to the oxidation of X^{2-} or X_n^{2-} at CdX. Over the potential range scanned the potential of the Pt electrode was invariant at −0.95 V vs. SCE and −1.05 V vs. SCE in the Se^{2-}/Se_n^{2-} and Te^{2-}/Te_2^{2-} electrolytes, respectively. It is gratifying to note that these potentials correspond to the literature values for the redox potential, E_{redox}, of the given X^{2-}/X_n^{2-} species.[31,33b] Likewise, in the polysulfide electrolyte we found the Pt potential to be at −0.72 V vs. SCE and again equal to the known value of E_{redox} for S^{2-}/S_n^{2-}.[33] In a general way the current-voltage curves are consistent with the model for semiconductor electrodes[26] in that no anodic current is observed in the dark. But photogeneration of the minority charge carrier (in this case, holes, h+) results in photocurrent. Dark cathodic currents are possible, but we have avoided cathodic current flow, since the reduction of the CdX could occur.

For the Se^{2-}/Se_n^{2-} electrolyte there are several trends worth noting. First, at a given light intensity, the potential onset for photoanodic current follows the ordering CdTe > CdS > CdSe with CdTe most negative. Second, the effect of light intensity is to vary the potential onset for photocurrent, with the higher light intensities giving the more negative onset. Moreover, the higher light intensities result in current-voltage curves that are somewhat less sharp (current rises less steeply). Trends in the Te^{2-}/Te_2^{2-} electrolyte are similar to those found in the Se^{2-}/Se_n^{2-} electrolyte, but the high light intensities apparently do not result in such misshaped curves. The onset potential does move more negative with increased light intensity and at a given light intensity the onset potential for photocurrent is more negative for CdTe than for CdSe.

The trends in the Se^{2-}/Se_n^{2-} and Te^{2-}/Te_2^{2-} electrolytes are comparable to those in the polysulfide electrolyte.[4,5] The onset potentials for photocurrent for CdS and CdSe were very similar with CdSe perhaps slightly more negative. The significance of the onset potential for photocurrent flow is twofold. First, it should establish the open-circuit photopotential at a given set of conditions. Second, the most negative onset (at highest light intensity) should approximately correspond to the flat-band potential, E_{FB}, of the semiconductor. The E_{FB} concept will be elaborated more fully below, but at least one can appreciate that the onset potential is of value in determining maximum output voltage, E_V. The value of E_V should be equal to $|E_{redox} - E_{FB}|$. For a value of Φ_e of unity and irradiation at E_{BG}, the efficiency for optical to electrical energy conversion is just E_V/E_{BG}, or for any Φ_e the efficiency is $(\Phi_e)(E_V/E_{BG})$. Our measures of energy conversion efficiency are detailed below.

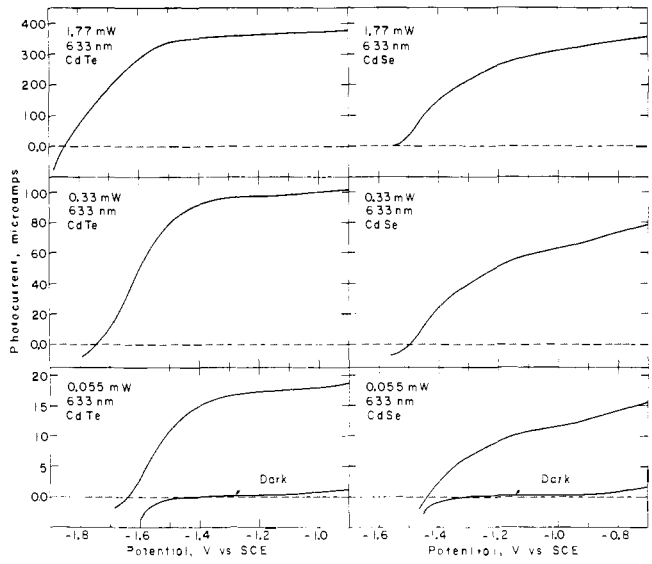

Figure 5. Current-voltage curves for CdSe and CdTe in ~10^{-2} M Te^{2-}/Te_2^{2-} in 5.0 M NaOH. The irradiated area is 0.25 cm^2. The Pt dark electrode was at a constant potential of −1.05 V vs. SCE (Te^{2-}/Te_2^{2-} potential) for all values of potential shown for the CdX electrode. These are potentiostated curves recorded at 2 mV/s.

2. Energy Conversion Efficiency. To measure *sustained* optical to electrical energy conversion efficiency of CdX-based photoelectrochemical cells employing X^{2-}/X_n^{2-} electrolytes, we have taken[4,5] the expedient of using a variable power supply in series in the external circuit as the electrical load. Thus, when the negative lead of the power supply is attached to CdX and the positive lead to Pt, the power *output* of the cell is just the applied negative potential, V_{appl}, times the photocurrent. The conversion efficiency is just electrical power output divided by the optical input power. The optical power in was measured using a calibrated radiometer as described in the Experimental Section. Table II summarizes our findings for the various combinations of photoelectrode and electrolyte.

Table II gives observed Φ_e values at the potential where the power output maximizes and also at the minimum load where Φ_e is maximum. Generally, for the cases shown the maximum value of Φ_e is observed near short-circuit. That is, in a no load situation the value of Φ_e is as high as ever observed. In the main, assisting the photoeffect (applying a *positive* bias) does not improve the value of Φ_e. Generally, the value of Φ_e is significantly below 1.0, but in many cases the Φ_e exceeds 0.50. The discrepancy between the Φ_e observed and unity can be rationalized by a number of points including (i) the electrolyte absorption; (ii) reflection losses; and (iii) inherent h^+-e^- recombination rates vs. interfacial electron transfer rates. However, the observed Φ_e values are respectable. Even at high light intensity the values of Φ_e remain high and we note relatively little saturation for the intensities given in Table II. The maximum conversion efficiency measured ranges from ~1 to ~14% with output voltages of 0.15-0.50 V at the maximum power output.

Table II. Optical to Electrical Energy Conversion Efficiency for CdX-Based Photoelectrochemical Cells

Crystal[a]	Electrolyte (T, °C)[b]	Irradiation λ, nm (intensity, mW/cm²)	Max power out, mW/cm²	η_{max},[c] %	V at η_{max}[d]	Φ_e at η_{max}[e]	Φ_e max[f] (V_{appl})
CdTe	0.18 M Se^{2-} (83)	633 (0.34)	0.028	8.2	0.30	0.54	0.71 (0.00)
		(1.24)	0.112	9.0	0.35	0.51	0.72 (0.00)
		(6.80)	0.624	9.2	0.35	0.51	0.73 (0.00)
CdTe	0.18 M Te^{2-} (49)	633 (0.224)	0.020	8.8	0.30	0.58	0.82 (0.00)
		(1.32)	0.130	10.0	0.30	0.65	0.77 (0.00)
		(7.08)	0.644	9.1	0.35	0.51	0.65 (0.00)
		(2.91)	0.273	9.4	0.35	0.53	0.66 (0.00)
		(25.7)	2.05	8.0	0.35	0.45	0.63 (0.00)
		(301)	14.4	4.8	0.45	0.21	0.32 (0.00)
		(519)	17.1	3.3	0.45	0.14	0.21 (0.00)
CdSe	0.18 M Se^{2-} (83)	633 (0.34)	0.0052	1.5	0.15	0.20	0.40 (0.05)
		(1.24)	0.0196	1.6	0.15	0.21	0.36 (0.05)
		(6.80)	0.144	2.1	0.20	0.20	0.35 (0.05)
CdSe	0.18 M Te^{2-} (49)	633 (2.80)	0.041	1.5	0.10	0.31	0.57 (0.00)
		(24.3)	0.375	1.5	0.15	0.20	0.35 (0.00)
		(298)	3.7	1.2	0.20	0.12	0.21 (0.00)
		(504)	5.5	1.1	0.25	0.08	0.15 (0.00)
CdS	0.09 M Se^{2-} (69)	501.7 (1.04)	0.030	2.9	0.20	0.36	0.47 (0.00)
		(4.40)	0.148	3.4	0.25	0.42	0.49 (0.00)
CdS	0.10 M Te^{2-} (60)	488 (0.348)	0.0045	1.3	0.15	0.22	0.36 (0.05)
		(1.76)	0.0252	1.4	0.15	0.24	0.33 (0.05)
		(14.4)	0.176	1.2	0.20	0.15	0.25 (0.05)
		(90.8)	0.592	0.7	0.20	0.08	0.12 (0.05)

[a] Cf. footnote *a*, Table I. [b] Cf. footnote *b*, Table I. [c] (Maximum electrical power out divided by optical power) × 100. [d] Output voltage at maximum power conversion efficiency. [e] Quantum efficiency for electron flow at the point of maximum power conversion efficiency. [f] Maximum quantum efficiency for electron flow. The V_{appl} value refers to the minimum applied potential from a power supply in series in the circuit needed to observe maximum photocurrent.

The optical to electrical energy conversion efficiencies reported here for CdTe-based cells are fairly attractive. The overall solar energy to electrical energy conversion is calculated to be a little greater than 5% in optimum cases. This represents the best efficiency to date for any wet photoelectrochemical device.

d. Determination of Flat-Band Potential: Open-Circuit Photopotential and Differential Capacitance Measurements. According to Gerischer,[26] the semiconductor-electrolyte interface should be as sketched in Scheme II for the dark and

Scheme II. Energy Levels of Semiconductor Near Electrolyte Interface

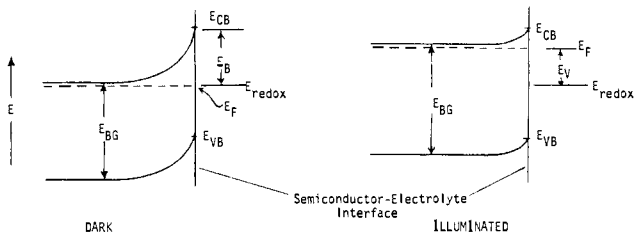

illuminated electrode at open circuit. In principle, the amount of band bending, E_B, is equal to the initial difference in the Fermi level, E_F, of the semiconductor and the value of E_{redox}, which is the potential of the reaction occurring at the electrode. The depletion region of the semiconductor resulting from the initial mismatch of E_F and E_{redox} allows for the inhibition of recombination of photogenerated h^+-e^- pairs. This provides a rationale for efficient photocurrents on semiconductors. The maximum value of E_V is equal to E_B. Thus, knowing E_{redox} one can establish the value of E_F when the bands are not bent. This is the so-called flat-band condition and the associated potential is the E_{FB} mentioned above. We can often take $E_{FB} \cong E_{CB}$, since the values of E_F and E_{CB} are nearly equivalent for heavily doped *n*-type materials. The positions of E_{CB} and E_{VB} at the surface are constant, for a given electrolyte. Thus, E_{FB} ultimately allows evaluation of the surface energy levels of the semiconductor and their relationship to E_{redox}. This is crucial, since for an oxidation to occur at the photoelectrode E_{VB} must be below E_{redox}, but a good overlap of E_{VB} with E_{redox} is theoretically needed for fast electron transfer. We have already noted that the onset potential for photoanodic current at the highest light intensity can be a good measure of E_{FB}. We now report open-circuit photopotentials as a function of light intensity for the various electrode/electrolyte combinations toward establishing the maximum value of E_V. Additionally, we report differential capacitance data which give an independent measure of E_{FB}.

1. Open-Circuit Photopotentials. Figure 6 shows open-circuit photopotentials, E_V, for all nine combinations of CdX and X^{2-}/X_n^{2-} electrolytes as a function of light intensity. The value of E_V is the light-induced potential difference between CdX and Pt under illumination of CdX at open circuit, measured with a high impedance voltmeter. In every case the potential difference between CdX and Pt was determined to be zero in the dark before and *after* the data were collected for a given electrode. For the lowest light intensities there is a linear relationship between E_V and log (light intensity). At the highest light intensities there is a saturation of the photopotential, which we take as reflecting the maximum value of E_V.

For the Te^{2-}/Te_2^{2-} and Se^{2-}/Se_n^{2-} electrolytes the CdTe photoelectrode gives a significantly higher E_V than CdSe or CdS. In the polysulfide electrolyte, though, the maximum value of E_V is within 0.12 V for each CdX. The E_V values and their light intensity dependence, overall, are in accord with E_V values obtained from current-voltage curves.

2. Differential Capacitance Measurements. Plots of differential capacitance vs. electrode potential have long been used to determine E_{FB} values.[34] We have carried out such measurements to determine the E_{FB} values for the various $CdX/X^{2-}/X_n^{2-}$ combinations. Also, linear plots of (differential capacitance)$^{-2}$ against potential (Mott-Schottky plots) allow evaluation of the donor density, N_D. The differential capacitance, C, should behave according to the equation

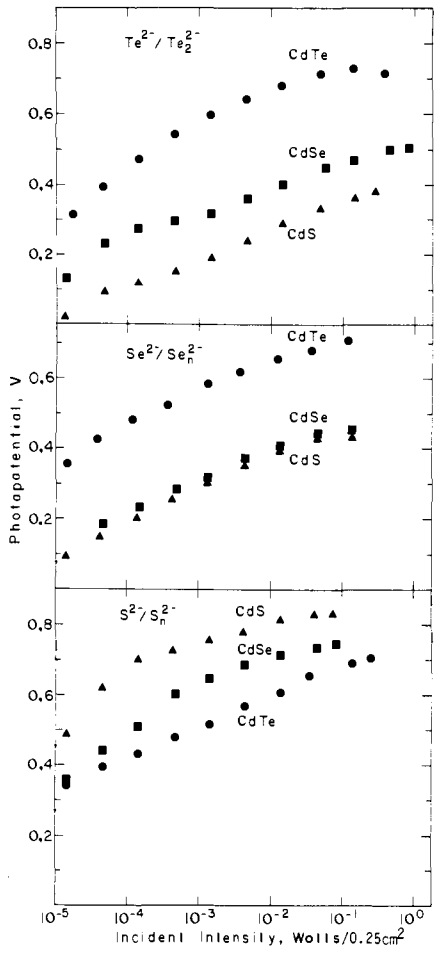

Figure 6. Open-circuit photopotential vs. incident optical power for CdX in the various X^{2-}/X_n^{2-} electrolytes. The irradiated area was 0.25 cm^2.

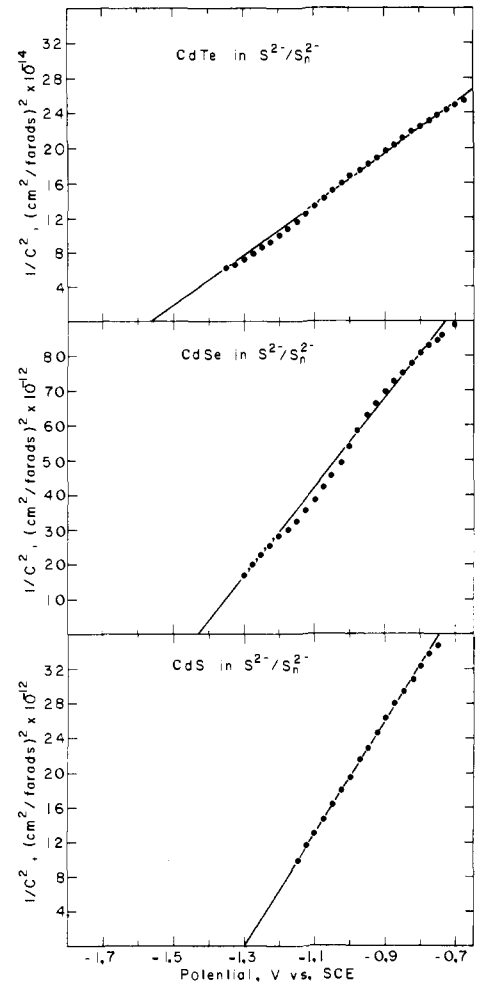

Figure 7. Representative plots of (differential capacitance)$^{-2}$ vs. CdX potential in the S^{2-}/S_n^{2-} electrolyte. The intercept represents the value of the Fermi level where the flat-band condition obtains.

$$\frac{1}{C^2} = \left(\frac{2}{\epsilon\epsilon_0 e N_D}\right) E_B \qquad (6)$$

where E_B is the band bending in the semiconductor which depends linearly on the potential, ϵ is the dielectric constant of the semiconductor, ϵ_0 is the permittivity of vacuum, and e is the absolute value of electron charge.

Representative plots of (differential capacitance)$^{-2}$ against potential for CdX (X = S, Se, Te) in the 1.0 M NaOH, 1 M S, 1 M Na_2S electrolyte are given in Figure 7. Similar data, comparable in quality, were obtained for CdX in Se^{2-}/Se_n^{2-} and Te^{2-}/Te_2^{2-} electrolytes. Additionally, we made the measurements in an electrolyte of 1.0 M K_2SO_4 with variable amounts of added NaOH or H_2SO_4 to change the pH from 12.7 to 4.8.

The values of E_{FB} (V vs. SCE) and N_D from the differential capacitance data are included in Table III. First, the data show the N_D is in the range of 4×10^{15}-2×10^{18} cm^{-3} for the semiconductors used in this study. These values are in accord with the calculated value from the resistivity and mobility for these semiconductors.

The significant results from the differential capacitance data concern the value of E_{FB}. We find a large difference in E_{FB} in the X/X^{2-} electrolyte compared to the value measured in the aqueous electrolytes containing no chalcogenide other than oxygen. As has been reported for CdS,[35] we find that E_{FB} for CdX is independent of pH. Incidentally, we measured E_{FB} for CdS in K_2SO_4 aqueous electrolyte to be −0.9 V vs. SCE independent of pH. This is in good agreement with the reported value −0.8 V vs. SCE.[35,36]

3. Assignment of Band Positions. The open-circuit photopotentials, the differential capacitance data, and the current-voltage curves at the highest light intensity enable us to evaluate E_{FB}, and hence, E_{CB} and E_{VB} can be calculated. We calculate for our electrodes that E_{FB} is within 0.1 V of E_{CB}, and consequently we will take $E_{CB} = E_{FB}$. Table III lists the values of E_{CB} and E_{VB} for the various electrolytes used in our studies. The three measures of E_{FB} are in good agreement, except for the case of CdTe in Se^{2-}/Se_n^{2-} and in Te^{2-}/Te_2^{2-}. In the latter two cases we find that the value of E_{FB} from both the photopotential and the current-voltage curves is more negative than that indicated from the capacitance measurements. If the model in Scheme II is correct, we must have E_B no less than the maximum measured value of E_V. For this reason we adopt, as the most accurate value, the value of E_{FB} from the photopotential and current-voltage curves for the CdTe.

e. Relationship of Band Positions and Electrolyte Redox Levels: Evidence for Important Kinetic Factors in Interfacial Electron Transfer. According to the model for photoelectrochemical action, the value of E_{redox} must be above the E_{VB} position in order to expect electron transfer from the redox active species to the photogenerated hole at the surface of the n-type semiconductor. For each CdX, in any of the X^{2-}/X_n^{2-} electrolytes or in O_2/OH^-, the position of E_{VB} is significantly below E_{redox}. Thus, the energetic requirement is apparently met by any aqueous electrolyte. However, the oxidation of H_2O to O_2 is not found for any of the three CdX n-type electrodes,

Table III. Band Positions for CdX Electrodes in X/X^{2-} Electrolytes[a]

Semiconductor (donor density,[b] cm^{-3})	Electrolyte[c]	From open-circuit photopotential		From current-voltage curves		From capacitance data[d]	
		$E_{FB} = E_{CB}$	E_{VB}	$E_{FB} = E_{CB}$	E_{VB}	$E_{FB} = E_{CB}$	E_{VB}
CdS	H_2O/OH^-					−0.90[e]	1.50
(5×10^{15}-5×10^{17})	S^{2-}/S_n^{2-}	−1.52	0.88	−1.20	1.20	−1.25	1.15
	Se^{2-}/Se_n^{2-}	−1.40	1.00	−1.47	0.93	−1.40	1.00
	Te^{2-}/Te_2^{2-}	−1.50	0.90			−1.40	1.00
CdSe	H_2O/OH^-					−0.70[e]	1.00
(3×10^{16}-2×10^{18})	S^{2-}/S_n^{2-}	−1.45	0.25	−1.40	0.30	−1.45	0.25
	Se^{2-}/Se_n^{2-}	−1.40	0.30	−1.42	0.28	−1.40	0.30
	Te^{2-}/Te_2^{2-}	−1.55	0.15	−1.55	0.15	−1.45	0.25
CdTe	H_2O/OH^-					−0.80	0.60
(4×10^{15}-2×10^{16})	S^{2-}/S_n^{2-}	−1.40	0.00			−1.50	−0.10
	Se^{2-}/Se_n^{2-}	−1.65	−0.25	−1.65	−0.25	−1.45	−0.05
	Te^{2-}/Te_2^{2-}	−1.80	−0.40	−1.85	−0.45	−1.50	−0.10

[a] All values shown are in volts vs. SCE. [b] Range of the donor density for samples used. Value is determined from slope of (differential capacity)$^{-2}$ vs. potential, cf. eq 6 of text. Dielectric constants for CdS, CdSe, and CdTe used were 5.2, 5.8, and 7.2, respectively; J. A. van Vechten, *Phys. Rev.*, **182**, 899 (1969). [c] S^{2-}/S_n^{2-} is 1.0 M S, 1.0 M Na_2S, 1.0 M NaOH. Se^{2-}/Se_n^{2-} is 5.0 M NaOH and 0.006-0.03 M total Se_n^{2-} added initially as Na_2Se. Te^{2-}/Te_2^{2-} is 5.0 M NaOH and 0.02-0.18 M total Te_n^{2-} added initially as Na_2Te. H_2O/OH^- is 1.0 M K_2SO_4 with pH of 4.8-12.7 achieved by adding appropriate amounts of NaOH or H_2SO_4. The temperature for H_2O/OH^- experiments was 298 K. For the X^{2-}/X_n^{2-} the temperature range was 298-355 K. [d] These values represent the average obtained from several determinations. [e] Cf. also ref 35 and 36.

nor do we find efficient oxidation of S^{2-} to S_n^{2-} at CdTe. Where we fail to obtain the energetically feasible oxidation we find instead photoanodic dissolution of CdX according to eq 1. The main point here is that the energetics are a necessary, but not sufficient, criterion to observe a given photoassisted process. The instability of CdTe in O_2/OH^- or S^{2-}/S_n^{2-} is particularly striking, since the E_{VB} and E_{redox} levels are nearly as close as in either the Te^{2-}/Te_2^{2-} or Se^{2-}/Se_n^{2-} electrolyte. The data demand the conclusion that kinetic factors are an important consideration in determining whether a given oxidation reaction will obtain.

It is interesting to consider the potential for the anodic dissolution of the CdX species. Latimer[37] gives a potential for S + $2e^-$ + Cd^{2+} → CdS of 0.08 V (vs. SCE), and we similarly calculate values of 0.29 and −0.14 V vs. SCE for CdSe and CdTe, respectively. We take these values to mean that if the crystal is held at a potential value more positive than that given, then the anodic dissolution is thermodynamically possible. Additionally, if holes are photogenerated in the VB of the *n*-type CdX where E_{VB} is more positive than the values given, then the photoanodic dissolution can occur. For every aqueous electrolyte-CdX combination studied the photoanodic dissolution is feasible, with the possible exception of CdTe in Se^{2-}/Se_n^{2-} and Te^{2-}/Te_2^{2-}. For situations where the photoanodic dissolution and the oxidation of the *added* chalcogenide or polychalcogenide are *both* possible, the energy levels are not a useful guide to whether one or the other will dominate, and kinetic factors must be invoked to account for the results.

The large energetic separation of E_{VB} and E_{redox} in the cases where we do find oxidation of the added X^{2-} or X_n^{2-} species is surprising. To account for the apparent fast interfacial electron transfer rates in these situations, we can invoke the concept of "surface states".[38] That is, there may be states located between E_{VB} and E_{CB} which establish good overlap with E_{redox}. This concept is sketched in Scheme III below. A similar proposal[27a,38] has been offered for *n*-type metal oxides. A fact that must seemingly be incorporated into this picture is that the surface states are very sensitive to, or dependent on, the electrolyte. Continued study of the CdX-electrolyte interface is needed to establish the nature of the surface states and factors influencing the rate of photoinduced electron transfer under energetically favorable conditions. We note that a recent study has found an empirical correlation of E_{redox} position and the ability of the electroactive additive to quench photoanodic dissolution of CdS.[39] Fast interfacial electron transfer was found for E_{redox} significantly more negative than the E_{VB} position. The instability of irradiated CdTe in S^{2-}/S_n^{2-} may be consistent with this correlation. The E_{redox} for S^{2-}/S_n^{2-} is not as far negative as E_{redox} for Te^{2-}/Te_2^{2-} or Se^{2-}/Se_n^{2-}.

Scheme III. Role of Surface States

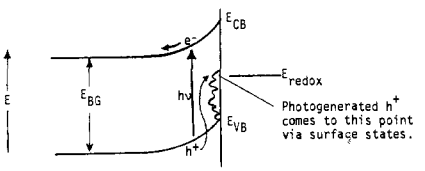

Experimental Section

Materials. CdS, CdSe, and CdTe single crystals were obtained as 10 × 10 × 1 mm plates from Cleveland Crystals, Inc. The 10 × 10 mm surface was oriented perpendicular to either the *c* axis (CdS and CdSe) or to the (111) plane (CdTe). Resistivities were measured by Cleveland Crystals, Inc. (four point probe method) to be 2-6 Ω-cm, 0.1-14 Ω-cm, and 1 Ω-cm for CdS, CdSe, and CdTe, respectively.

Electrolytes. Preparation of polysulfide electrolyte was performed under an Ar purge due to the solution's air sensitivity. The electrolyte was prepared by the addition of 0.1 mol each of NaOH, $Na_2S \cdot 9H_2O$ (Mallinckrodt), and sublimed sulfur (Baker) to 100 mL of Ar-purged distilled water. Solutions of Se^{2-} and Te^{2-} were prepared from Na_2Se and Na_2Te by modifying the method of Tschugaeff and Chlopin.[40] Both the solids and their aqueous solutions are extremely air sensitive and Schlenk techniques were employed in all stages of their handling.

In a typical preparation ~1.0 g of Se (Baker, reagent grade) or Te powder (American Smelting and Refining Co.) and 4.0 g of $Na_2S_2O_4$ (Fisher) were added to 50 mL of Ar-purged 10% NaOH. The solution was heated to ~70 °C and turned brown or purple as Se_n^{2-} or Te_2^{2-}, respectively, was formed. After about 30 min the solution cleared, indicating complete reduction to Se^{2-} or Te^{2-}. As the solution cooled, white crystals of Na_2Se or Na_2Te precipitated. After filtration the crystals were washed three times with cold 10% NaOH to remove any remaining $Na_2S_2O_4$. Any attempt to completely dry the crystals resulted in the formation of some colored polyselenide or ditelluride. Stock solutions were prepared by simply dissolving Na_2Se or Na_2Te in Ar-purged 5 M NaOH. The total concentration of selenide (Se^{2-} and Se_n^{2-}) and telluride (Te^{2-} and Te_2^{2-}) was determined gravimetrically by exposing a known volume of the solution to air and

weighing the precipitated element. Yields of Na_2Se and Na_2Te were ~80% based on Se or Te, respectively. The room temperature solubility of Na_2Se and Na_2Te was 0.005 and 0.03 M, respectively. Solutions of selenide and telluride are stable indefinitely, even at elevated temperatures, if rigorously protected from air.

Electrodes. Prior to being mounted as electrodes, CdX crystals were cut to ~5 × 5 × 1 mm and etched. CdS was etched for 1 min in concentrated HCl; CdSe was etched by a mixture of HNO_3, H_2SO_4, CH_3COOH, and HCl (30:20:10:0.1 by volume) at 50 °C for 8 s, then rinsed, first by concentrated H_2SO_4, then by water; the etchant for CdTe was a mixture of 6 g of $Na_2Cr_2O_7 \cdot 2H_2O$, 15 mL of concentrated HNO_3, and 50 mL of H_2O into which the crystal was immersed at 25 °C for 1 min. After etching, a gallium-indium eutectic was rubbed on one face of the crystal and this was placed on a glass encased copper wire whose end had been coated with silver epoxy. All exposed metal was then insulated with ordinary epoxy.

Cells. Experiments in polysulfide electrolyte were performed in a Pyrex vessel 3 cm in diameter and 9-cm long. The solution was stirred and purged by bubbling Ar through it. Extreme air sensitivity precluded the use of this method for solutions of selenide or telluride. Instead, a tube 3.2 cm in diameter, 12-cm long, with a side arm above the solution level was employed. The top of the cell was fitted with a rubber stopper containing holes for a 9 cm × 1 mm diameter Pt wire (to which a 2 × 4 cm Pt gauze was attached), an SCE, the semiconductor, and a vent.

The solution was stirred and heated, if required, by positioning it on a Corning stirrer-hot plate. Ar was continuously passed over the solution via the side arm after having been bubbled through a reservoir of distilled water in order to maintain solution volume. Standard three electrode geometry was used for all potentiostated experiments (the photoanode was always placed as close to the wall of the cell as possible). For all experiments not requiring an SCE, a two-hole rubber stopper (Pt, photoelectrode) was used.

Optics. The semiconductors were irradiated with several sources. Monochromatic irradiation at 632.8 nm was provided by a Spectra Physics He-Ne laser and at 514.5, 501.7, and 488.0 nm by a Spectra Physics argon ion laser. A 6× beam expander was used to expand the 1-mm (He-Ne) and 1.5-mm (argon ion) diameter beams. Intensity was varied with colored filters and/or adjustment of laser power. Visible and near IR monochromatic irradiation was also obtained by passing the output of a 650-W GE tungsten halogen lamp through a Bausch and Lomb 33-86-77 high intensity monochromator. The full output of this lamp was often used for stability experiments; its UV output was removed with a Corning 3-73 filter and infrared irradiation was absorbed by passing the beam through 18 cm of H_2O. Light intensity was measured with a Tektronix J16 digital radiometer equipped with a J6502 probe. A beam splitter was employed in experiments requiring continuous monitoring of light intensity.

Current-Voltage Curves. A PAR 174 polarographic analyzer was used in conjunction with an HP 7040A x-y recorder to obtain curves where the photoanode was potentiostated against an SCE. Standard three-electrode geometry was used. A second kind of current-voltage curve was obtained with an HP 6241 power supply in series with the photoanode and a 10 × 2 cm strip of Pt gauze. Curves of photocurrent vs. applied potential were obtained in this manner, the current being measured as the potential drop across a 10 or 100 Ω resistor in series in the circuit. Light intensity was obtained with the Tektronix radiometer.

Wavelength Dependence. Monochromatized light from the tungsten halogen lamp was used to determine relative photocurrent as a function of excitation wavelength. After the lamp's intensity between 450 and 900 nm was calibrated with the Tektronix radiometer, photocurrent at zero bias was obtained for CdTe in optically clear Na_2Te electrolyte as a function of wavelength. Photocurrent was then corrected for the variation in light intensity. Analogous data for CdS and CdSe in sulfide electrolyte was previously reported.[4] The optical spectrum of a 1-mm thick sample of CdTe was measured after polishing both faces of the crystal with 0.1 μm alumina. The spectrum was recorded on a Cary 17.

Quantum Yields. Quantum yields for electron flow were measured for all stable electrode electrolyte combinations (Table II). Beam-expanded laser beams were masked so as not to exceed the exposed crystal surface area, and photocurrent as a function of applied potential (see circuit under Current-Voltage Curves) was measured. The Tektronix radiometer measured light intensity simultaneously by means of a beam splitter.

Open-Circuit Photopotential. A high impedance HP 7101B strip chart recorder, placed in series with the photoelectrode and Pt gauze, measured the open-circuit potential. Laser lines at 501.7 and 514.5 nm were beam expanded and masked to just fill the photoelectrode surface. Light intensity was monitored with the Tektronix radiometer in conjunction with a beam splitter. Values of open circuit photopotential were obtained for all nine electrode/electrolyte combinations.

Stability. Electrolyte stability was established by following visible-UV spectral changes on the Cary 17 of the two Pt electrolysis of Na_2X solution. The electrolyses were carried out in 0.1- or 1.0-mm optical cells from Precision Cells, Inc. An analogous photoassisted electrolysis of Na_2Te solution with CdTe was performed in a stoppered 13 × 100 mm test tube with a side arm. The photoelectrode and Pt gauze were suspended in the solution from an air-tight hole in the stopper. Spectral changes were recorded by placing the entire assembly in the Cary 17 sample chamber.

Electrode stabilities were measured under a variety of conditions (see Table I). Crystals were weighed (±0.1 mg) after etching, prior to mounting. After long-term irradiation the crystals were demounted by removing the epoxy with CH_2Cl_2 and weighed again.

Flat-Band Potentials. Capacitance measurements were recorded at 1 kHz with an HP 4260A universal bridge. The bias voltage was applied (HP 6241A power supply) through the bridge leads between the Pt and semiconductor electrodes; the potential difference between the anode and the SCE was monitored with a Data Precision 1450 digital multimeter. The capacitance was recorded in 25-mV steps over the ranges as shown in Figure 7, with equilibration after each voltage increment. Experiments were performed in the dark; all nine electrode electrolyte combinations were studied.

Acknowledgment. We thank the National Aeronautics and Space Administration for support of this research. Support from the M.I.T. Cabot Solar Energy Fund is also gratefully acknowledged.

References and Notes

(1) John and Fannie Hertz Foundation Fellow.
(2) Fellow of the Alfred P. Sloan Foundation, 1974-1976, and recipient of a Dreyfus Teacher-Scholar Grant, 1975-1980.
(3) A. B. Ellis, S. W. Kaiser, and M. S. Wrighton, *J. Am. Chem. Soc.*, **98**, 1635 (1976).
(4) A. B. Ellis, S. W. Kaiser, and M. S. Wrighton, *J. Am. Chem. Soc.*, **98**, 6855 (1976).
(5) A. B. Ellis, S. W. Kaiser, and M. S. Wrighton, *Adv. Chem. Ser.*, in press.
(6) A. B. Ellis, S. W. Kaiser, and M. S. Wrighton, *J. Am. Chem. Soc.*, **98**, 6418 (1976).
(7) (a) G. Hodes, J. Manassen, and D. Cahen, *Nature (London)*, **261**, 403 (1976); (b) B. Miller and A. Heller, *ibid.*, **262**, 680 (1976).
(8) H. Gerischer and W. Mindt, *Electrochim. Acta*, **13**, 1239 (1968).
(9) G. Hodes, D. Cahen, and J. Manassen, *Nature (London)*, **260**, 312 (1976).
(10) A. Fujishima and K. Honda, *Bull. Chem. Soc. Jpn.*, **44**, 1148 (1971); *Nature (London)*, **238**, 37 (1972).
(11) M. S. Wrighton, D. S. Ginley, P. T. Wolczanski, A. B. Ellis, D. L. Morse, and A. Linz, *Proc. Natl. Acad. Sci., U.S.A.*, **72**, 1518 (1975).
(12) J. Keeney, D. H. Weinstein, and G. M. Haas, *Nature (London)*, **253**, 719 (1975).
(13) A. J. Nozik, *Nature (London)* **257**, 383 (1975).
(14) J. H. Carey and B. G. Oliver, *Nature (London)*, **259**, 554 (1976).
(15) W. Gissler, P. L. Lensi, and S. Pizzini, *J. Appl. Electrochem.*, **6**, 9 (1976).
(16) T. Ohnishi, Y. Nakato, and H. Tsubomura, *Ber. Bunsenges. Phys. Chem.*, **79**, 523 (1975).
(17) K. L. Hardee and A. J. Bard, *J. Electrochem. Soc.*, **122**, 739 (1975).
(18) J. G. Mavroides, D. I. Tchernev, J. A. Kafalas, and D. F. Kolesar, *Mater. Res. Bull.*, **10**, 1023 (1975).
(19) A. Fujishima, K. Kohayakawa, and K. Honda, *Bull. Chem. Soc. Jpn.*, **48**, 1041 (1975); *J. Electrochem. Soc.*, **122**, 1437 (1975).
(20) L. A. Harris and R. H. Wilson, *J. Electrochem. Soc.*, **123**, 1010 (1976).
(21) M. S. Wrighton, A. B. Ellis, P. T. Wolczanski, D. L. Morse, H. B. Abrahamson, and D. S. Ginley, *J. Am. Chem. Soc.*, **98**, 2774 (1976).
(22) J. G. Mavroides, J. A. Kafalas, and D. F. Kolesar, *Appl. Phys. Lett.*, **28**, 241 (1976).
(23) T. Watanabe, A. Fujishima, and K. Honda, *Bull. Chem. Soc. Jpn.*, **49**, 355 (1976).
(24) M. S. Wrighton, D. L. Morse, A. B. Ellis, D. S. Ginley, and H. B. Abrahamson, *J. Am. Chem. Soc.*, **98**, 44 (1976).
(25) A. B. Ellis, S. W. Kaiser, and M. S. Wrighton, *J. Phys. Chem.*, **80**, 1325 (1976).
(26) H. Gerischer, *J. Electroanal. Chem.*, **58**, 263 (1975), and references cited therein.
(27) (a) J. M. Bolts and M. S. Wrighton, *J. Phys. Chem.*, **80**, 2641 (1976). (b) A recent paper on *n*-type Fe_2O_3-based cells shows that visible response can

be obtained, but with significant deterioration of current-voltage properties: K. L. Hardee and A. J. Bard, *J. Electrochem. Soc.*, **123**, 1024 (1976); **124**, 215 (1977).
(28) D. Dutton, *Phys. Rev.*, **112**, 785 (1958).
(29) R. G. Wheeler and J. Dimmock, *Phys. Rev.*, **125**, 1805 (1962).
(30) (a) R. H. Bube, *Phys. Rev.*, **98**, 431 (1955); (b) D. A. Jenny and R. H. Bube, *ibid.*, **96**, 1190 (1954); (c) J. Camassel, D. Auvergne, H. Mathieu, R. Triboulet, and Y. Marfaing, *Solid State Commun.*, **13**, 63 (1973).
(31) (a) J. J. Lingane and L. W. Niedrach, *J. Am. Chem. Soc.*, **70**, 4115 (1948); (b) A. J. Panson, *J. Phys. Chem.*, **67**, 2177 (1963).
(32) Reference 31a includes redox behavior of Se^{2-}, including the claim that the oxidation product is Se_2^{2-}.
(33) (a) P. L. Allen and A. Hickling, *Trans. Faraday Soc.*, **53**, 1626 (1957); (b) W. M. Latimer, "Oxidation Potentials", 2nd ed, Prentice Hall, New York, N.Y., 1952.
(34) (a) J. F. DeWald, *Bell Syst. Tech. J.*, **39**, 615 (1960); (b) H. Gerischer in "Physical Chemistry", Vol. IXA, H. Eyring, D. Henderson, and W. Jost, Ed., Academic Press, New York, N.Y., 1970, Chapter 5.
(35) T. Watanabe, A. Fujishima, and K. Honda, *Chem. Lett.*, 897 (1974).
(36) (a) Reference 34b, p 485; (b) V. A. Tyagai and G. Ya. Kolbasov, *Surf. Sci.*, **28**, 423 (1971); (c) E. C. Dutoit, R. L. Van Meirhaeghe, F. Cardon, W. P. Gomes, *Ber. Bunsenges. Phys. Chem.*, **79**, 1206 (1975).
(37) Reference 33b, p 174.
(38) "Surface states" located between the valence and conduction band have been detected optically in photoelectrochemical cells employing aqueous electrolytes for SnO_2: H. Kim and H. Laitinen, *J. Electrochem. Soc.*, **122**, 53 (1975); and for CdS: C. E. Byvik, Abstracts, Electrochemical Society Meeting, Washington, D.C., April 1976, No. 238; cf. also S. N. Frank and A. J. Bard, *J. Am. Chem. Soc.*, **97**, 7427 (1975).
(39) T. Inoue, K. Kohayakawa, T. Watanabe, A. Fujishima, and K. Honda, submitted for publication and private communication.
(40) L. Tschugaeff and W. Chlopin, *Ber.*, **47**, 1269 (1914).

Study of *n*-Type Gallium Arsenide- and Gallium Phosphide-Based Photoelectrochemical Cells. Stabilization by Kinetic Control and Conversion of Optical Energy to Electricity

Arthur B. Ellis,[1] Jeffrey M. Bolts, Steven W. Kaiser, and Mark S. Wrighton*[2]

Contribution from the Department of Chemistry, Massachusetts Institute of Technology, Cambridge, Massachusetts 02139. *Received September 27, 1976*

Abstract: We report herein the behavior of *n*-type GaAs- and GaP-based photoelectrochemical cells employing alkaline aqueous solutions of chalcogenide and polychalcogenide ions, X^{2-} and X_n^{2-} (X = S, Se, Te). For GaAs in Te^{2-}/Te_2^{2-} and GaP in Se^{2-}/Se_n^{2-} or Te^{2-}/Te_2^{2-}, the photoanodic dissolution of the GaAs or GaP photoelectrode does not occur; rather, the chalcogenide is oxidized at the photoelectrode. Other combinations of GaAs or GaP photoelectrodes and X^{2-}/X_n^{2-} electrolytes give photoanodic dissolution of the photoelectrode, despite the fact that chalcogenide oxidation is still energetically feasible. The results support the conclusion that kinetic factors, not energetics alone, control whether a given X^{2-}/X_n^{2-} electrolyte will be oxidized at the photoelectrode at a rate which precludes photoanodic dissolution of the electrode. For any case where the photoelectrode is stable, it is possible to sustain conversion of optical energy to electricity. Wavelengths shorter than those corresponding to the band gaps of 2.24 and 1.35 eV for GaP and GaAs, respectively, are effective. Conversion efficiencies for monochromatic light are a few percent, with output voltages of ~0.2–0.45 V at the maximum power output. Sustained conversion is possible because the photoelectrode is stable and also because the electrolyte undergoes no net chemical change, since the substance oxidized at the photoelectrode is reduced at the dark counter electrode.

Much attention is now turning to photoelectrochemical cells[3] as a means of converting optical energy to chemical fuels[4-15] and/or electricity.[16-21] In the preceding paper[20] and elsewhere[16-19] we have established that the photoanodic dissolution of *n*-type semiconductors CdX (X = S, Se, Te) can be quenched by competitive electron transfer from electroactive substances in the electrolyte. Such stabilization of photoelectrodes is also being studied in other laboratories,[21] and it is now quite evident that certain electroactive reagents can be oxidized at irradiated *n*-type electrodes with no other side reactions. For the stabilization of CdX by X^{2-} (X = S, Se, Te), we have further established that the oxidation product (X_n^{2-}) is reducible at the counter electrode to regenerate X^{2-}. The chemistry can be represented as in the reactions

$$A \rightarrow A^+ + e^- \quad \text{(photoanode)} \qquad (1)$$

$$A^+ + e^- \rightarrow A \quad \text{(cathode)} \qquad (2)$$

We have demonstrated that one can exploit such schemes to sustain the efficient conversion of low-energy visible light to electricity, when photoinduced current passes through a load in the external circuit.

A key to further advances in using semiconductor photoelectrochemistry is to elaborate the factors controlling whether the interfacial oxidation of a species A will compete with the photoanodic dissolution of an *n*-type semiconductor. Curiously, for example, CdTe is susceptible to photoanodic dissolution in the presence of S^{2-}, whereas both CdSe and CdS are stable. We showed[20] that S^{2-} oxidation at irradiated CdTe is energetically feasible, but apparently the rate is too slow to completely quench another energetically feasible process corresponding to photoanodic dissolution.

In order to understand the factors controlling interfacial electron transfer at the photoelectrodes, we have pressed to find new examples of quenched photoanodic dissolution. In this paper we report the first stabilization of *n*-type GaP (E_{BG} = 2.24 eV)[22] and GaAs (E_{BG} = 1.35 eV)[23] by the competitive electron-transfer technique using chalcogenide ions as reductants. Both of these *n*-type semiconductors are well known to undergo photoanodic dissolution in aqueous electrolytes.[24-27] We think it noteworthy that these materials are shown to be stabilized by certain chalcogenide ions, but do not themselves contain chalcogenide lattice ions.

Results and Discussion

The sections below detail our characterization of *n*-type GaAs and GaP photoelectrodes in cells employing chalcogenide/polychalcogenide, X^{2-}/X_n^{2-} (X = S, Se, Te) electrolytes. Unless stated otherwise, the solvent is 5.0 M NaOH, and all results have been obtained in cells blanketed under Ar with stirred electrolytes. For three of the six possible combi-